From Zero-Stiffness to Neutral Stability Using Stress Relaxation

Matthias Blaakman and Giuseppe Radaelli(✉)

Delft University of Technology, Mekelweg 5, 2628 CD Delft, The Netherlands
g.radaelli@tudelft.nl

Abstract. This paper presents a novel prestressing method for polymeric compliant zero-stiffness mechanisms to obtain neutral stability. The method utilizes stress relaxation as an actor for imprinting a permanent elevated internal stress state. The method in question does not require a complex mechanical setup for application of the prestress. An existing zero-torsional stiffness mechanism is presented as a case study to demonstrate the working principle. Simulations have been performed and experimentally validated to present how stress relaxation can induce neutrally stable behavior in zero-stiffness compliant mechanisms. A sensitivity analysis is performed for the relaxation time to see its influence on the shift of the moment-angular deflection curve.

Keywords: Neutral stability · zero-stiffness · prestress · viscoelasticity · stress relaxation · creep · compliant mechanisms

1 Introduction

In the field of compliant mechanisms, the most often used materials are polymers due to their high yield strength to Young's modulus ratio [3]. One of the biggest obstacles in working with polymers is their inherent viscoelastic behavior. Viscoelastic effects such as stress relaxation occur at any level of deformation induced stress, at room temperature, in polymers [4]. It can severely impact the predictability of polymeric mechanisms' behavior.

One of the main objectives of compliant mechanisms is mimicking the functionality of regular joints. Where typical joints have no preferred configuration as long as their internal friction is overcome, compliant mechanisms struggle on this front. The obvious reason for this is that the bending and twisting of material results in a reaction force attempting to undo the deformation. All techniques that are employed to neutralize this elastic restoring force, i.e. obtaining elastic neutral stability, require a form of prestress to be introduced into the system, whether it consist of connecting a positive and a negative stiffness element together, or whether it is applied to a monolithic structure. The process of prestressing is often a difficult balancing act. Especially monolithic structures are difficult to enable to behave neutrally stable. Where creating neutrally stable monolithic structures is usually limited to very simply shaped mechanisms,

E. Lanteigne and S. Nokleby (Eds.): CCToMM M3 2025, 184, pp. 87–97, 2025.
https://doi.org/10.1007/978-3-031-95489-4_8

for example the tape spring from Murphey and Pellegrino [6] or the coiled strip from Seffen and Guest [8], the prestressing method presented in this paper is also applicable to more complex shapes.

This paper shows how, based on two criteria, a zero-stiffness mechanism can be transformed into a neutrally stable mechanism utilizing the viscoelastic phenomenon stress relaxation. It enables for a transformation of monolithic zero-stiffness mechanisms with complex geometry into neutrally stable mechanisms, using a novel prestressing method. The prestressing method is referred to as the stress relaxation prestressing (SRPS) method.

The paper continues with the method section, in which the method of applying prestress using stress relaxation will be explained in combination with an example: a helicoidal shell joint. In this section also a numerical model, used to predict the behavior for a given deformation and relaxation, is presented. Furthermore, the experimental setup to validate the model in question is also shown. The results section will follow, showing the neutral stability of the mechanism through the SRPS method. The discussion and conclusion section, will reflect on the obtained results, along with an attempt to explain discrepancies between the numerical model and the experimental results. Some recommendations for future research will also be given here.

2 Method

Before diving into prestressing method, a few concepts are explained to give a better understanding as to what is happening during the prestress process. Firstly, stress relaxation is shortly addressed. Then, we explain the idea of using stress relaxation as a means of applying prestress. Here two requirements for mechanisms for which this method is suitable are stated. Then, the mechanism that is being prestressed is presented, explaining how it adheres to the stated requirements. Finally, the numerical model and experiments are presented.

2.1 From Zero-Stiffness to Neutral Stability

For regular zero-stiffness mechanisms, the force-deflection curve looks somewhat similar to the initial deformation (ID) phase of Fig. 1(a), with a constant force-level of a. Here the force can be interpreted in a generalized sense, where in a rotational system it would signify a moment. If the system is deformed from its initial configuration to a deformed configuration, such as at the end of the ID phase, a set amount of work has to be done. If the mechanism in question is held in its deformed position for an extended amount of time, see the relaxation phase of Fig. 1, the internal stresses will dissipate through stress relaxation and therefore the force on the mechanism will drop to zero at some point in time. Since there is no more restoring force, the mechanism will not deform back to its initial state. Releasing the mechanism at this point in time, its internal rearrangements will have led to this configuration being the new 'preferred' configuration of the system. If the deformed configuration of the mechanism would be a near mirror

image of the original configuration, it would be expected that the force-deflection curve inverts when the new preferred configuration is assumed. The reason for this is that a mechanism, when fully relaxed after deforming it to its mirror image configuration, would behave as if it was fabricated in this mirrored configuration. As such, the zero-stiffness region would have vertically shifted from a force value of a to a value of b, where $b = -a$, as can be seen in the figure in the returning deformation (RD) phase. What this means in practice is that now the system will require a set amount of work to move from the deformed configuration back to the initial configuration, as it no longer tends to move back to its initial state by itself. The hypothesis that is derived from these observations is whether there is also a point in time where the mechanism is deformed and relaxed, but not yet to the point that the zero-stiffness region has shifted from a to b, but rather from a to 0, as depicted in the RD phase in Fig. 1(b), rendering the mechanism neutrally stable.

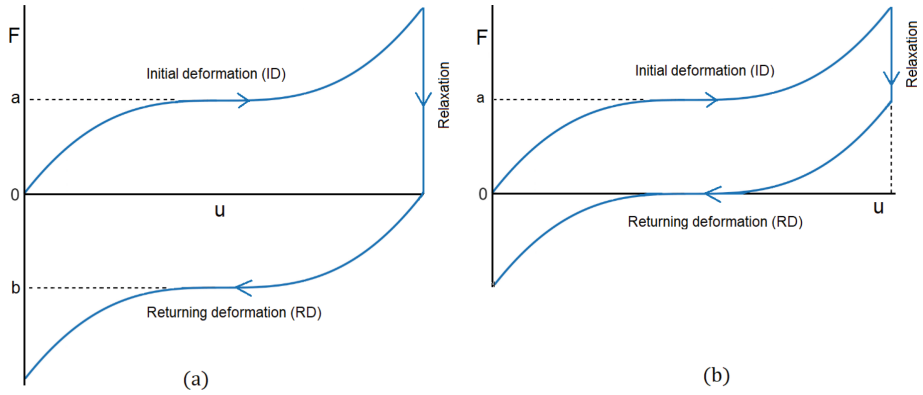

Fig. 1. Force-deflection curve of generic zero-stiffness mechanism with full relaxation (a) and partial relaxation (b).

Following the rationale above, a set of two requirements emerges for a compliant mechanism be made neutrally stable using the SRPS method:

1. The mechanism can be deformed in a way that its deformed configuration is a near mirror image of its undeformed configuration.
2. The mechanism has a zero-stiffness region.

The first criterion stems from the fact that a relaxation phase in a non-mirrored configuration might lead to a whole different curve in the RD phase, meaning that the system will no longer be neutrally stable if it ever were zero-stiffness. This would also imply that mechanisms which are not zero-stiffness in the first place might still become neutrally stable when using the SRPS method, however the investigation of this thought is left for future research.

The second criterion only gives an initial shape to a shifting curve on the force/moment axis of the force-displacement/moment angular deflection diagram. If this curve can be made to retain its original shape, making the assumption that a mirrored relaxation phase does not alter the mechanism's slope, the system will become neutrally stable after the relaxation phase.

2.2 Case Study: Helicoidal Shell Joint

In order to show that the proposed idea applies to a complex example, the zero-stiffness helicoidal shell joint designed by Radaelli [7] has been chosen as a case study to be made neutrally stable. Radaelli presents the synthesis of a helicoidal shell structure consisting of 6 flanges, attached at a symmetry axis, see Fig. 2(a). The exact geometry has been adopted for this paper with height h = 0.1 m, width w = 0.01 m, pitch angle $\theta = 180°$, and flange thickness t = 0.4 mm (not shown), see Fig. 2(b).

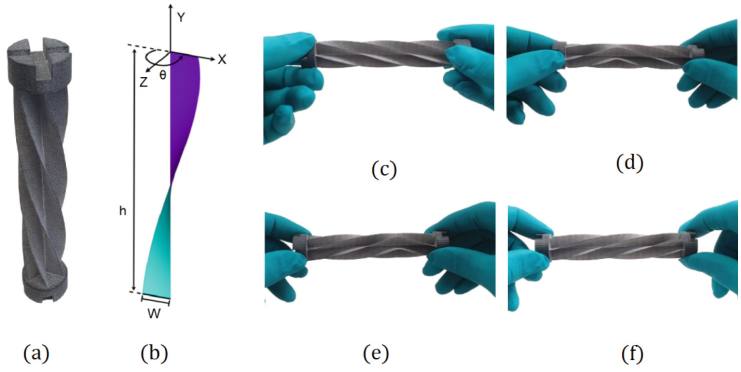

Fig. 2. A helicoidal shell compliant joint [7] (a), a schematic of the helicoidal reference geometry (b), and the deformation propagation (c)–(f).

When taking a look at the helicoid, it is visible that the twisting of the mechanism around its symmetry axis results in a mirrored version of the original, especially if you compare Fig. 2(c) and Fig. 2(f).

The mechanism derives its zero-stiffness from the fact that when one end is clamped and the other is rotated around its symmetry axis, after the initial buckling region, the only deformation happening is a propagation and extension of the flipped region along its length. Therefore, a constant amount of work is being done when rotating further. For the full deformation to a mirrored configuration, see Fig. 2(c)–(f).

2.3 Numerical Model Helicoidal Shell Joint

The geometry of the helicoidal shell joint was created using Solidworks 2023, and imported in Ansys Mechanical APDL 2022 R2, using the Parasolid command. A

static structural analysis was performed on the geometry. The helicoid's numerical model has been reduced to a single helicoid, instead of the 6-helicoid physical sample, and constrained on the middle axis to account for the axisymmetry. The geometry is meshed with four node SHELL181 element type. Due to the high levels of deformation in the material, Nylon (PA12) was chosen for the helicoid. The helicoidal samples were created using multi-jet fusion (MJF) 3D printing.

The material properties can bee seen in Table 1. The material model consists of a combination between a viscoelastic material model, and a linear elastic material model. In a viscoelastic model, this spring is put in parallel with one or multiple sets of spring-damper components. In the table, the Young's modulus and Poisson ratio, E and ν respectively, are the linear elastic parameters and have been adopted from Radaelli's paper [7], since the helicoid has been made at the same manufacturer using the same material and manufacturing process.

In order to model the viscoelastic behavior we need the relationship between the shear relaxation modulus and time for our material. For this, a 5th order Prony series curve fit has been made of experimental stress relaxation test data. A tensile test bench has been used to extend a dog bone-like structure. The dog-bone is stretched to ˜105% of its free length, from 30 mm to 31.5 mm, and then held at that specific length for a set period of time. This is similar to the ID- and relaxation phases of the SRPS method. Curve fitting the data using the Prony series curve fit, gives the relaxation modulus $E(t)$.

Making the assumption that the material in question is nearly incompressible due to the fact that most of the deformation in the material comes from the shearing of the polymeric chains [2], enables for deriving a direct relationship between the general relaxation modulus, $E(t)$, and the shear relaxation modulus, $G(t)$, given as:

$$G_0(t) = \frac{E_0(t)}{2(1+\nu)} = \frac{E_0}{3}. \tag{1}$$

In Table 1, constants $\alpha_0 - \alpha_5$ and $\tau_1 - \tau_5$ are called Prony constants describing at what specific time what a specific amount of decay has occurred.

Additionally, to introduce temperature sensitivity, the William-Landel-Ferry (WLF) shift function for the material need to be determined. The WLF shift function relies on the time-temperature superposition principle and determines how temperature changes affect the relaxation of material. The WLF shift function is given as

$$\log(a_T) = -\frac{C_1(T - T_{ref})}{C_2 + (T - T_{ref})}, \tag{2}$$

in which $log(\alpha_T)$ is the shift function, C_1 and C_2 are constants determined from testing a multitude of temperatures, T_{ref} is the reference temperature to which a variation in relaxation is compared, and T is the operating temperature for the tests. The constants C_1 and C_2 have been derived from curve fitting data from the literature [1]. The use of the WLF relationship is only valid when the material is thermorheologically simple, or more simply stated, if it adheres to the Time-Temperature superposition principle (TTS).

Table 1. Material properties helicoidal shell joint, including linear elastic material properties, Prony constants and WLF constants.

Parameter	Value	Unit
E	1.8e9	Pa
v	0.38	–
refT	20	°C
C1	60	–
C2	280	°C
α_0	0.9	–
α_1	0.85	–
α_2	0.71	–
α_3	0.63	–
α_4	0.55	–
α_5	0.508	–
τ_1	10	s
τ_2	1.00e2	s
τ_3	1.00e3	s
τ_4	1.00e4	s
τ_5	2.40e4	s

The boundary conditions of the system consist of both imposed displacement and a body force load in the form of an imposed temperature. The imposed temperature highly influences the degree of stress relaxation and is therefore used to match the experimental and numerical results. All nodes in the model are given a body force load in the form of a temperature of 18 °C. In the simulation shown in Fig. 3, the line at the far end on the left (green) is constrained in all DoFs. The line on the far end of on the right (red) is constrained in translation along the x- and z-axis, and in rotation around the x- and z-axis. The symmetry axis (blue) is constrained in rotation around the x-axis and z-axis. A small distorting moment has also been applied near the top line (double arrow) in order to initiate buckling at a specific location. Not including the buckling moment would result more simulation difficulty due to the arising of a singularity. In the physical model the initiation of buckling is of no concern because of manufacturing imperfections. In 10 time steps, the top line (red) is rotated around the symmetry axis (blue), held for a specific relaxation time, and rotated back, in again 10 time steps. The helicoid has been simulated for a variation in relaxation time. The tests were performed for relaxation times from 1000 s to 4000 s, while keeping the rotation constant at 360°, which is exactly mirrored around the symmetry axis.

An additional test is performed by going through the ID, relaxation and RD phases, and on top of that two additional ID-RD cycles. This test is to verify

that a lowered constant moment level is retained also after the first prestressing cycle.

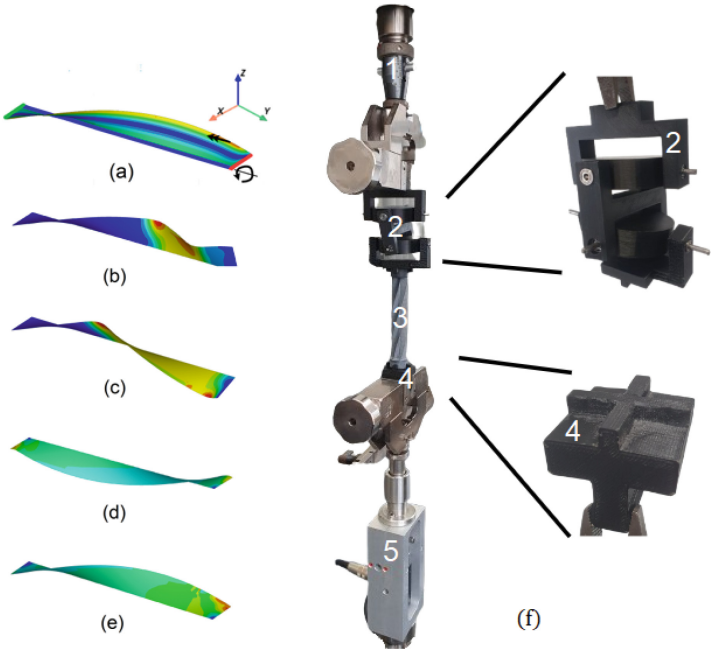

Fig. 3. Helicoidal shell simulation fully undeformed (a), to partially deformed (b) (c), to fully mirrored (d) and back (e), and experimental setup (f) with rotating clamp (1), attached to cardan axis (2), clamped to helicoid (3), on top of a PLA block (4) in a clamp attached to a load cell (5).

2.4 Experimental Validation Helicoid

In order to validate the proposed method and the numerical results of the helicoidal shell model, a torque test has been performed utilizing a torque bench, consisting of a rotating clamp, attached to a cardan-joint to alleviate alignment issues, in which the helicoidal compliant joint is clamped, which is fixed on the bottom side to a stationary load cell, see Fig. 3(f). The hardware includes a ZwickRoell torque test and tensile test bench combination with a HBM T20WN load cell.

The experiments for the helicoidal shell include, to mimic the simulation, a variation in relaxation time, from 1000 s to 4000 s, while keeping the rotation at 360°. The upper clamped part, attached to the cardan axis, is rotated around its longitudinal axis in the ID phase, held during the relaxation phase and then rotated back in the RD phase. The torque bench rotated the upper attachment with an angular speed of 36°/s.

3 Results

In this section, the experimental results are presented to see if, firstly, the tested mechanism indeed does become neutrally stable. And secondly, to gauge the predictive value of the numerical simulation. The results are presented in the form of moment-angular deflection curves, which include both the numerical and experimental results for a single ID, relaxation and RD cycle. The goal is to asses the influence of relaxation time on the degree of stress relaxation and therefore the moment reduction. It is good to note that temperature is not directly taken into account as a testing variable, but merely as a model parameter taken from the environment. Performing an experiment in which the temperature could be varied would require a more sophisticated experimental setup with a climate chamber.

The experimental results of the varying relaxation time test can be found in Fig. 4(a). As can be seen in the figure, the model and the experiment match relatively closely, but the height of the second peak on the ID phase seems to be lower in the measured samples. In a zoomed version of the figure, Fig. 4(b), a close match between the numerical and experimental data can be observed. Thus, for a variation in relaxation times, the numerical model for the helicoidal shell seems to be a good predictor of the stress relaxation behavior when the helicoid is deformed.

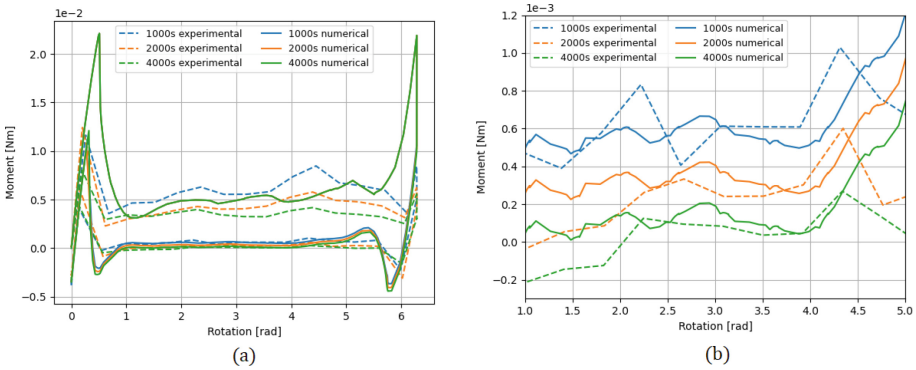

Fig. 4. Moment-angular deflection curve helicoidal shell for a variation of relaxation time.

Besides the close match between theoretical and physical results, it is clear as well that there is a major difference in torque between ID and RD phase. For a relaxation time of 4000 s, the torque level in the zero-stiffness region of the RD phase is a fraction $\frac{M_{back}}{M_{forth}} = \frac{0.1Nmm}{4.0Nmm} = 0.025$ of the torque in the ID phase. Thus, the constant moment-level during the RD phase is reduced by about a factor 40. This model is therefore indeed capable of predicting the required time to make the helicoidal shell joint neutrally stable. The result of this experiment

can also be visually observed on the physical model, see Fig. 5, in which the helicoidal shell joint no longer has a preferred configuration.

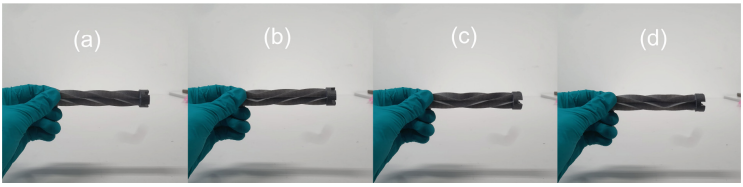

Fig. 5. Neutrally stable helicoid in multiple positions.

Another important result is displayed in Fig. 6, showing that the drop in torque is maintained on the short term through repeated cycles. In this figure, first the mechanism is deformed, relaxed and deformed back (ID1, relaxation and RD1 phases). Afterwards, the mechanism is deformed and deformed back two more times (ID2, RD2, ID3, RD3 phases). The upper line shows the ID phase of the first deformation of the mechanism. The lower lines show the RD phase after relaxating the mechanism for 8000 s. And the middle two lines again show the ID phase after the relaxation has taken place. What this shows is that after relaxation, the band in which the mechanism operates is lowered. As each cycle continues, the opacity of the figure is lowered to give a clearer representation. It can be noticed that for this specific sample after 8000 s the band did drop significantly, but not below the 0 Nm line like the sample used for Fig. 4.

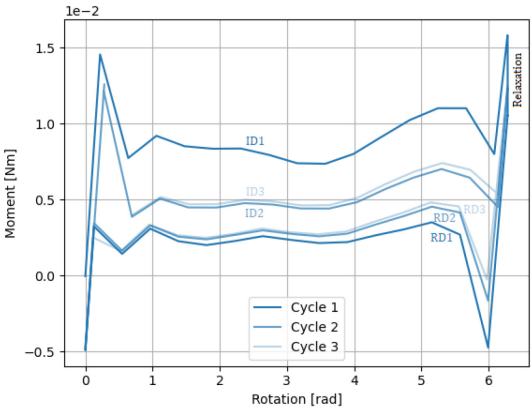

Fig. 6. Experimental moment-angular deflection curve for multiple cycles after 8000 s relaxation.

4 Discussion and Conclusion

This section will reflect on the results of Sect. 3 and address some limitations of this research. This paper focuses on the transformation of a generic zero-stiffness (ZS) mechanism into a neutrally stable mechanism by using stress relaxation as a prestressing actor. The test results indicate that increasing relaxation time results in a further downward shifted moment level in the RD phase. An explanation for this would be that since the monomers have a longer time to untangle and shear, the level of relaxation will increase. The model for the helicoid seems to reasonably match the test results. It also shows that both the ID and RD phase after relaxation hoover around a limit, lower than the original constant moment level, when repeatedly deformed and undeformed. The discrepancy between Fig. 4 and Fig. 6 in moment level after relaxation might stem from the fact that the latter test has been performed months later than the first test series. As a result, extra crosslinking might have occurred in the test samples, decreasing the amount of relaxation they undergo for a set amount of time. Additionally, the temperature of the experiment, the accumulation of moisture over time and imperfections in the sample itself may also have contributed to this difference.

One of the limitations of this research is the fact that the Prony series data is limited. As mentioned before, a test setup in which the test temperature could be controlled was too complex for the purposes of this research. As a result, the Prony series data could only be gathered for a single temperature, a room temperature of 18°C. Recalling the WLF, a slight increase in temperature at deformation can lead to a major increase in stress relaxation. If the experiments are to be done on a day warmer than about 25°C, the accelerated relaxation would saturate the simulation.

Another important point to make that is only implicitly addressed is the fact that all experiments and simulations take a finite amount of time to perform, ergo strain rate was not taken into consideration. The amount of time steps it took to complete the simulations was mostly dependent on the convergence needs and not precisely the same as in the experiment. This might lead to some slight deviations in the results.

The final point to address is the fact that only one zero-stiffness mechanism has been tested. There might be specific cases of zero-stiffness mechanisms in which the SRPS method does not work. A more extensive research on classifying zero-stiffness mechanisms and their ability to be made neutrally stable using this method should be done to emphasize the claims from this work.

To give some leads for further research concerning the use of stress relaxation for prestressing, a few suggestions will be made. Firstly, investigation of the potential of metals instead of polymers is recommended. Using polymers in this study was mostly done for the practicality of viscoelastic behavior at room temperature. Metals only exhibit this behavior when being stressed at high temperatures [5]. What this means is that if the SRPS method is applied for metals at a high temperature, letting it relax at this temperature, and the metal cools down again to room temperature, the neutrally stable behavior might be of more

permanent nature. This would largely expand the practical use of this concept to obtain neutrally stable compliant mechanisms. In broader sense, it would help compliant mechanisms to get rid of one of their primary disadvantages, namely their elastic spring-back.

A further expansion of this research could be to do the mentioned types of tests for a different temperature. The choice of what polymer to use would then not be limited to the glass transition temperature of the material.

Concluding, this work presents a novel prestressing method to create neutrally stable mechanisms from complex monolithic structures. The broad group of compliant mechanisms for which this method would be viable needs to have a zero-stiffness region in its intended deformation direction along with the ability to configure as a mirror image of its original configuration in this deformation direction.

The results section compares the numerical simulation and experimental results of the helicoidal shell. It was clear that in the helicoidal shell, neutral stability could be achieved by extending the relaxation phase of the SRPS method.

References

1. Amel, H.: Investigating the cyclic performance of laser sintered nylon 12. Ph.D. thesis, University of Sheffield (2015)
2. Ferry, J.: Viscoelastic Properties of Polymers, vol. 264. Wiley, Hoboken (1980)
3. Howell, L.L., Magleby, S.P., Olsen, B.M., Wiley, J.: Handbook of Compliant Mechanisms. Wiley Online Library, Hoboken (2013)
4. Hussein, E.K., et al.: Perspective chapter: viscoelastic mechanical equivalent models. In: Biomimetics-Bridging the Gap. IntechOpen (2022)
5. Kassner, M.: Fundamentals of Creep in Metals and Alloys. Elsevier/Academic Press (2015)
6. Murphey, T., Pellegrino, S.: A novel actuated composite tape-spring for deployable structures. In: 45th AIAA/ASME/ASCE/AHS/ASC Structures, Structural Dynamics & Materials Conference, p. 1528 (2004)
7. Radaelli, G.: Reverse-twisting of helicoidal shells to obtain neutrally stable linkage mechanisms. Int. J. Mech. Sci. **202**(106), 532 (2021)
8. Seffen, K.A., Guest, S.D.: Prestressed morphing bistable and neutrally stable shells (2011)